The influence of simultaneous mechanical and thermal loads on the stress distribution in molars with amalgam restorations

D. AROLA*, M.P. HUANG
Department of Mechanical Engineering, University of Maryland Baltimore County, 1000 Hilltop Circle, Baltimore, MD 21250, USA
E-mail: darola@engr.umbc.edu

A finite element analysis (FEA) of a mandibular molar restored with Class II amalgam restoration was conducted to determine the stress distribution which results from a superposition of simultaneous mechanical and thermal loading. A fully crossed three-level four-factor experimental design was used to evaluate the relative influence of crown temperature, time of thermal loading, occlusal force, and cavo-surface margin adhesion on the stress distribution. It was found that occlusal force and temperature had significant influence on the stress distribution and particularly on the maximum principal stress. Over the range in oral conditions considered, thermal loading contributed for over 35% of the stress within the restored molar subjected to simultaneous mechanical and thermal loads. Furthermore, thermal loading had significant effects on the magnitude of normal stress that develops parallel to the pulpal floor. Although marginal bonding of amalgam reduces the stress resulting from occlusal forces, thermal loading promotes the development of significant interfacial shear stresses along the bonded margin. Stresses related to the thermal component of loading concentrate near the pulpal floor and lingual surface margin, the site most prominent in cusp fracture. Hence, results from this study clearly indicate that an evaluation of new dental materials and/or restorative designs should consider the effects from a superposition of simultaneous mechanical and thermal loads on fracture resistance

1. Introduction

The failure of dental restorations due to fracture of the tooth or restorative material is a significant clinical problem. In fact, tooth fracture has been found to be one of the primary reasons for replacement of amalgam restorations [1]. Although the major causes for tooth loss are periodontal disease and caries, tooth fracture is also a major contributing factor. Furthermore, the probability of tooth fracture and/or cracking due to the degradation in restoration quality becomes much more prominent with age [2]. Consequently, tooth fracture has become an obstacle to maintaining lifelong oral health. In that regard, the fracture of restored teeth continues to be a problem of increasing clinical concern.

In an attempt to understand the mechanisms responsible for tooth fracture, the stress distribution within restored teeth that results from masticatory loading has been studied extensively. Early investigations were conducted using photoelasticity to examine specific aspects of cavity design on the resulting stress distribution [3, 4]. More recent efforts have relied on the use of finite element analysis to examine the effects from various factors on restoration failure; the majority of these have focused on the effects from cavity design and material parameters on the stress state that results from occlusal loads [5–7]. Of special interest are the numerical studies related to cavo-surface bonding which have identified the opportunity for reducing the strain and stress distribution, respectively, within intracoronal restorations [8, 9]. A significant number of related investigations have been reported, but a full review is far beyond the scope of this study.

Although the influence of cavity design on the stress distribution remains of clinical interest, more recent emphasis has been placed on the effects of restorative materials to restoration failure. For instance, comparisons in the clinical success of amalgam and composite dental restorations have received considerable attention. A comparison of the clinical success between MOD amalgam and resin fillings after 10 years from treatment showed that the cumulative survival rate of premolars with resin restorations was more than double that of premolars with amalgam restorations [10]. But in contrast to clinical assessments, experimental investigations on restored molars with Class I and II preparations have repeatedly shown that there is little difference in the fracture resistance provided by amalgam or composite restorations [11–13]. Therefore, due to the discrepancy

*Author to whom all correspondence should be addressed.

0957–4530

between clinical reports and results from experimental investigations, it appears that the nature of experimental evaluation to distinguish fracture resistance has not captured a critical component of the oral environment which contributes to restoration failure. In other words, occlusal loading which results from mastication may be only partially responsible for the majority of restoration failures.

While the influence of mastication and mechanical occlusal loads on the fracture of molars with restorations have been studied extensively, the influence of thermal loading has received far less attention. Differences in thermal properties between the biological and restorative materials promotes the development of stresses resulting from thermal expansion mismatch [14–16]. In fact, stresses in the tooth resulting from temperature changes have been found to be sufficient in magnitude to promote crack initiation in enamel [17, 18]. Although considered separately, the stress distribution within molars with amalgam restorations that results from a superposition of mechanical and thermal loads has not been reported. Simultaneous mechanical and thermal loading is a clinically relevant condition which may contribute to cusp fracture and/or tooth cracking. Therefore, an examination of the stress distribution in molars with amalgam fillings that results from simultaneous mechanical and thermal loading is warranted.

The purpose of this investigation was to determine the relative significance of both mechanical and thermal loads on the stress distribution which results in molars with amalgam restorations. A finite element analysis was used to model a mandibular molar restored with standard Class II amalgam restoration subjected to simultaneous mechanical and thermal loading. The stress distribution, including the location and magnitude of maximum principal stress, is reported in relation to effects from various oral factors. In addition, the significance of results from this study to amalgam restoration failures are discussed.

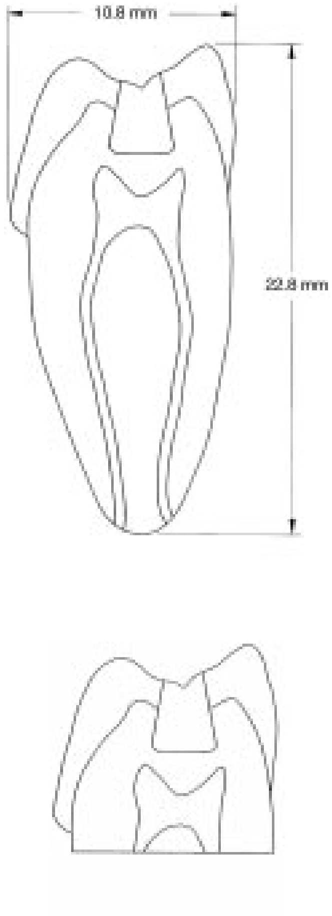

(a)

(b)

Figure 1 Schematic diagrams of the finite element models, (a) full model, (b) anatomic crown model.

2. Materials and methods

The stress distribution within a restored molar that results from either mechanical or thermal loading may be conveniently found using a finite element analysis (FEA). Consequently, a finite element model for a mandibular molar with standard Class II amalgam preparation was developed.

2.1. Finite element model

A finite element model was developed for an entire molar with Class II amalgam preparation and a crown molar with the same amalgam preparation, as shown in Fig. 1. A commercial computer-aided-design and finite element software was used to develop the model geometry and finite element mesh for both restorative designs [19]. The shape and dimensions of the molar were obtained from the permanent dentition traits reported in the literature [20]. As evident in Fig. 1, a symmetric amalgam configuration was chosen for this study. The overall restoration geometry is based on standard design convention [21]. The tooth and amalgam were meshed with four node plane strain isoparametric elements using an average element edge length of 0.25 mm along the cavity interface; note the mesh refinement near the dentin/amalgam and enamel/amalgam boundaries. The full tooth and crown models were comprised of 1737 and 1235 total elements, respectively. To ensure that an appropriate element size had been found for the analysis, a test for convergence of the temperature and stress distribution with element size was conducted.

According to the restoration configuration, mechanical properties of the constituents, and boundary conditions promoted by adjacent teeth, a plane strain analysis was considered most appropriate. During mastication, the maximum degree of deformation occurs in the buccal and lingual directions due to the cusp geometry. Elastic deformation along the mesial and distal axes is far smaller in comparison. Therefore, a plane strain analysis of the tooth is most consistent with the physical boundary conditions promoted by natural dentition. Material properties for the biological constituents and amalgam were obtained from a variety of sources. Properties for the dentin, pulp, and amalgam were obtained from a survey of the results reported and used by previous investigators [15, 22–24]. Each of these materials were assumed to exhibit isotropic behavior as reported. In contrast, the enamel was considered to be anisotropic according to a recently reported study [7]. Although the microstructural appearance of dentin suggests that it is mechanically anisotropic, the elastic modulus has not been found to be influenced by the dentinal tubule orientation. A recent evaluation of the shear strength in

TABLE I Material properties used in the finite element analysis

Property	Amalgam	Dentin	Enamel	Pulp
Mechanical				
E_1 (MPa)	50.0×10^3	20.0×10^3	80.0×10^3	2.07
E_2, E_3 (MPa)	n/a	n/a	20.0×10^3	n/a
v_{12}	0.29	0.31	0.30	0.45
v_{13}, v_{23}	n/a	n/a	0.08	n/a
Thermal				
$\rho(\text{kg/m}^3)$	10 500	1960	2800	1000
C_b (J/(kg · °C))	240	1600	712	4200
k (J/(m · s · °C))	22.70	0.59	0.93	0.67
α ((m/m)/°C)	2.50E–05	1.01E–05	1.15E–05	1.01E–05

directions parallel and perpendicular to the dentinal tubule orientation has shown that the degree of anisotropy is minimal [25]. Therefore, the dentin has been considered to be isotropic in the finite element model. A complete list of the mechanical and physical properties used for the finite element model is provided in Table I.

Following development of the meshed solid models, each model was translated into a second commercial finite element package [26] which permits an advanced treatment of surface interaction. Both the buccal and lingual interfaces were modeled using conditions which describe either perfect or imperfect bonding whereas the pulpal floor was considered to be bonded under all conditions of analysis. Perfect bonding required that both the tensile and compressive stress components normal to the cavo-surface margin remain continuous. In contrast, imperfect bonding conditions maintained only compressive stress continuity. In addition to bonding, Coulomb friction was introduced along the imperfect boundary to distinguish the contribution of mechanical interlocking promoted by tab preparation. The coefficient of friction μ was varied from 0 to 1.0. Friction was only applicable for simulations in which the margins were not assumed to be bonded.

Boundary conditions for both the complete molar and anatomic crown models were specified to maintain consistency with physiological conditions. The vertical and horizontal displacements of the full tooth surface nodes were assumed to be fixed according to support provided by the alveolar socket. Similarly, vertical displacement of the base nodes for the crown model were restricted but horizontal displacement was allowed to permit Poisson's expansion. A distributed load was specified for both models normal to the occlusal surface over 10 nodes of the lingual cusp. The distribution and orientation of occlusal loading is shown for the crown model in Fig. 2. Based on an average elemental length of 250 μm, the total masticatory load was delivered across 2.5 mm of the occlusal surface. The resultant force was varied from 0 to 200 N as per reports of occlusion from [27]. Thermal loads were applied to the tooth by specifying surface node temperatures along the entire anatomic crown. Temperatures between 5° and 55 °C were considered and the time of exposure was varied from 0 to 10 sec. The surface node temperatures were maintained at a constant value throughout the time of exposure. Actual temperatures within the mouth would begin to approach the intraoral temperature over time. The extent and rate of temperature change would depend on thermal properties and relative density of the consumed substance. Therefore, prescribing a constant temperature to the crown surface nodes over the entire duration of analysis represents the maximum extent of thermal loading. It should also be noted that the period of thermal loading in this investigation is much less than that used during experimental investigations conducted to examine the effects of thermal fatigue on teeth [28].

2.2. Design of numerical experiments

Due to the number of variables under consideration the numerical analysis was conducted according to a three-level, four-factor, nine-run experimental design; temperature, time of thermal loading, occlusal force, and cavo-surface margin coefficient of friction μ were the four independent variables chosen for the design of experiments. Table II contains the three levels of each independent variable used in this study. To produce a fully crossed experimental design array, three sets of nine runs were performed, consisting of a low, medium and high level nine-run set (27 numerical experiments). A full factorial analysis (consideration of all possible parametric combinations) would require 81 total simulations. In addition, the high level nine-run set was repeated using perfect bonding across the buccal and lingual cavo-surface margins. Therefore, a total of 36 separate simulations were conducted in which the stress distribution was recorded. For each stress state, the in-

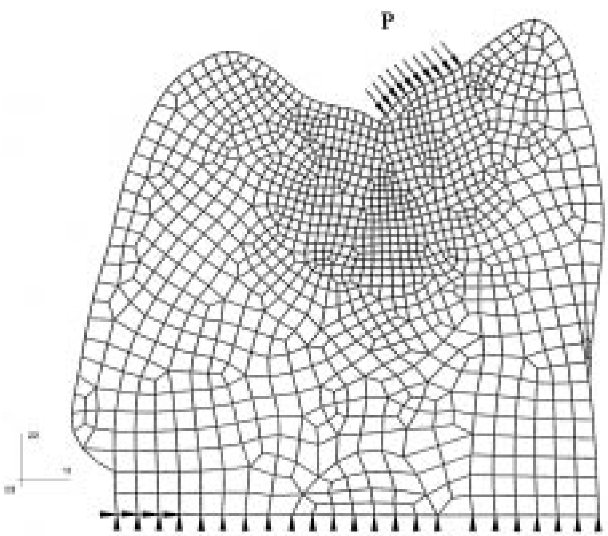

Figure 2 Boundary conditions for the anatomic crown model. The total occlusal load is represented by the magnitude P.

TABLE II Parametric levels of the independent variables

Level	Temperature (°C)	Time (s)	Occlusal Load (N)	Friction μ
Low	5	1	0	0.0
Medium	30	5	100	0.5
High	55	10	200	1.0

plane maximum principal stress was determined according to [29]

$$\sigma_1 = \frac{\sigma_{11} + \sigma_{22}}{2} + \left[\left(\frac{\sigma_{11} - \sigma_{22}}{2}\right)^2 + (\sigma_{12})^2\right]^{1/2} \qquad (1)$$

where σ_{11}, σ_{22}, and σ_{12} are the in-plane normal and shear stress components according to the coordinate definitions in Fig. 2. The in-plane principal stress is actually the maximum principal stress according to the convention $\sigma_1 > \sigma_2 > \sigma_3$. Following the numerical study, an analysis of variance (ANOVA) was used to determine relative effects of the oral parameters on the resulting stress distribution. An ANOVA can be used to distinguish the percentage contribution of each oral independent variable on the dependent variable of interest, namely the individual stress components. The relative per cent effect of each oral parameter was calculated by the ratio of the individual parametric sum of squares to the total sum of squares of all parameters. A review of experimental design and ANOVA can be found in [30].

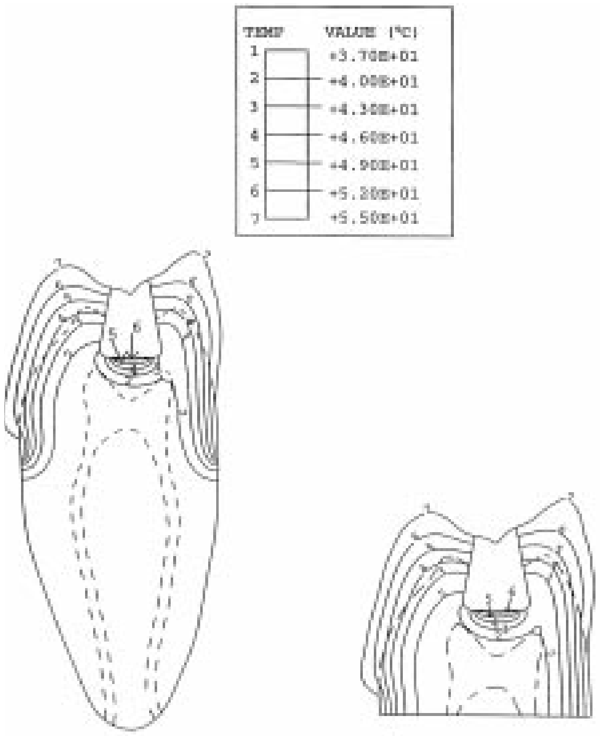

(a) (b)

Figure 3 Temperature distribution resulting from thermal loading of the models. ($T = 55\,°\mathrm{C}, t = 5\,\mathrm{s}$); (a) full model, (b) anatomic crown model. The dashed line is used to distinguish the boundary between the enamel, dentin and pulp.

3. Results

A finite element analysis of a mandibular molar with Class II amalgam restoration was used to determine the stress distribution resulting from a superposition of mechanical and thermal loading. The study was conducted according to a fully crossed three-level four-factor experimental design including the effects of temperature, time of thermal loading, occlusal force, and cavo-surface bonding. For each set of parametric conditions, a heat transfer analysis was necessary to identify the temperature distribution throughout the restored molar. The temperature distributions resulting from thermal loading for both the full tooth and crown models are shown in Fig. 3a and b, respectively. Each of the models in Fig. 3 were subjected to a an anatomic crown surface temperature of 55 °C for a period of 5 sec. The temperature distribution within the two models was found to be identical, regardless of the time of thermal loading. Therefore, in the interest of computational efficiency, the crown model was chosen for further study. Following the thermal analysis which was conducted according to the specific set of parametric conditions, a stress analysis was conducted with the appropriate occlusal load and interfacial friction. The temperature distribution resulting from thermal loading was written to a file which was then recalled during the stress analysis to simultaneously account for effects related to thermal expansion (or contraction). Utilizing the restored molar temperature distribution shown in Fig. 3b, the corresponding stress distribution for the anatomic crown model was computed while also accounting for the simultaneous application of a 100 N occlusal load and cavo-surface margin coefficient of friction equal to 0.5. Contour plots for each of the in-plane stress components σ_{11}, σ_{22}, and σ_{12} resulting from the aforementioned oral conditions are shown in Fig. 4 (a–c), respectively. The stress distribution presented in Fig. 4 was determined according to the conditions described for Experiment 3 listed in Table III.

TABLE III The stress distribution within the restored molar for oral conditions of the high level orthogonal array

Experiment	Temperature (°C)	Time (s)	Occlusal Load (N)	Interface (μ)	σ_{11} (MPa)	σ_{22} (MPa)	σ_{33} (MPa)	σ_{12} (MPa)	σ_1 (MPa)
1	55	10	200	1.0	8.43	− 0.16	− 6.76	13.92	18.70
2	55	1	0	0.0	7.34	2.04	− 4.74	3.52	9.10
3	55	5	100	0.5	8.10	1.31	− 5.65	10.71	15.94
4	5	5	200	0.0	1.68	− 4.68	− 6.48	17.97	16.75
5	5	10	0	0.5	2.90	1.69	− 2.80	1.86	4.25
6	5	1	100	1.0	0.11	− 5.27	− 8.80	8.06	5.92
7	30	1	200	0.5	3.26	− 6.28	− 8.36	1.47	3.48
8	30	5	0	1.0	3.71	1.22	− 5.53	2.49	5.25
9	30	10	100	0.0	4.11	− 0.83	− 5.76	7.80	9.82

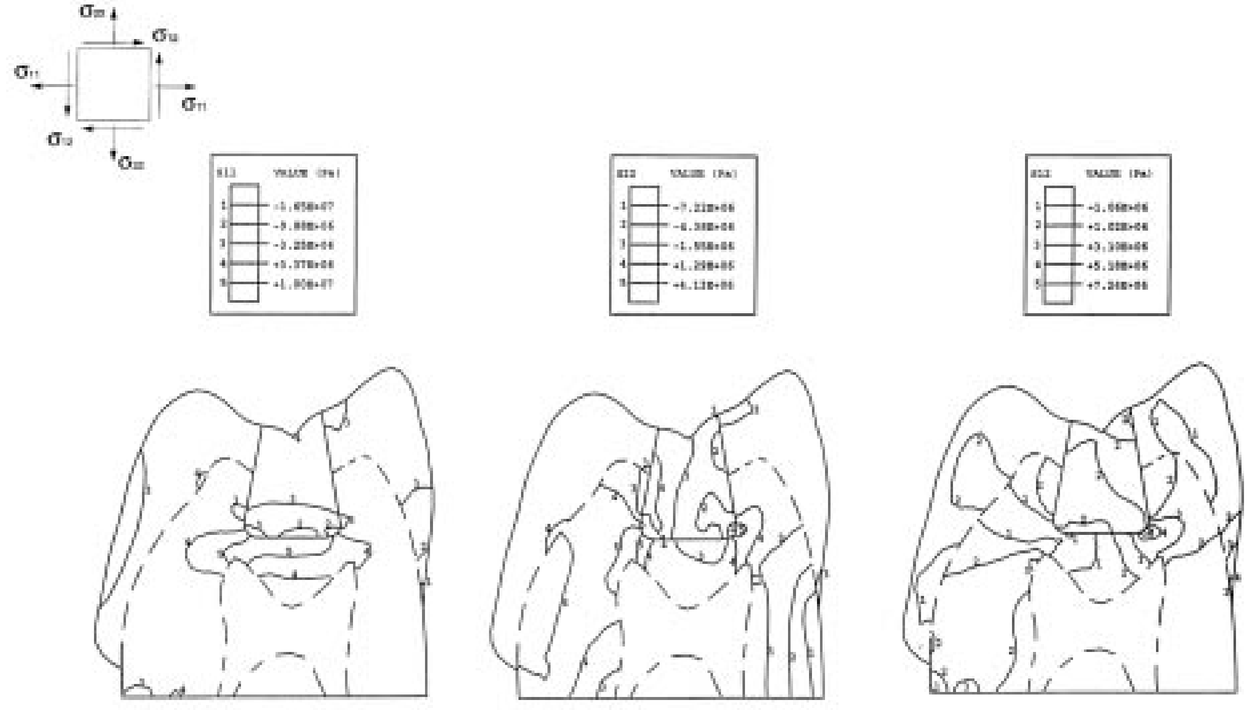

(a) (b) (c)

Figure 4 The stress distribution resulting from a superposition of mechanical and thermal loading. ($T = 55\,°\mathrm{C}, t = 5\,\mathrm{s}, P = 100\,\mathrm{N}, \mu = 0.5$); (a) σ_{11}, (b) σ_{22}, (c) σ_{12}. The dashed line is used to distinguish the boundary between the enamel, dentin and pulp.

For each set of oral conditions outlined by the design of numerical experiments, the location of maximum principal stress (σ_1) was identified and recorded. Interestingly, regardless of the oral conditions, the location of maximum stress was found to exist at the junction of the pulpal floor and lingual surface margin. The concentration of stress within this region is clearly evident from the distribution in stress components in Fig. 4. Numerical results for the maximum principal stress resulting from the nine conditions of the high level orthogonal array are listed in Table III. Note that the maximum stress reported for each condition in Table III was obtained at the junction of the pulpal floor and lingual surface margin. The maximum principal stress of all conditions of analysis was found to be 20 MPa and resulted when both the temperature and occlusal load were set to the high level as distinguished in Table II; the time of thermal loading and cavo-surface friction were at their low and medium levels, respectively.

Following completion of the fully crossed three-factor, four-level experimental design, an analysis of variance (ANOVA) was conducted to determine the relative contribution of each independent variable on the maximum principal stress. Note that the ANOVA was conducted using results from the low, medium, and high level experimental design for each stress component separately (σ_{11}, σ_{22}, σ_{33}, σ_{12}, and σ_1). Analysis of variance results from the three nine-run arrays were then averaged for a cumulative representation of the parametric effects from each independent variable; the averaged parametric effects are listed in Table IV. Thermal loading was found to be most influential on the in-plane normal stress σ_{11}, whereas occlusal loading had significant influence on the remaining in-plane components of stress (σ_{22}, and σ_{12}). Also clearly apparent was the significant contribution of both temperature and occlusal load on the maximum principal stress σ_1. In comparison, the effects of cavo-surface margin friction and the time of thermal loading are far less important.

TABLE IV Relative effects of the oral conditions on the maximum principal stress at the pulpal floor and lingual surface margin junction

Component	Temperature (% effect)	Time (% effect)	Occlusal load (% effect)	Friction (% effect)
σ_{11}	86.04	8.07	3.57	2.32
σ_{22}	18.06	14.51	63.34	4.09
σ_{33}	6.48	25.82	38.99	28.71
σ_{12}	4.46	4.03	90.77	0.75
σ_1	35.36	3.71	59.38	1.56

4. Discussion

A finite element analysis of a restored mandibular molar with Class II preparation was conducted. The effects of simultaneous thermal and mechanical loading on the stress distribution within the molar were examined. Thermal loads were distinguished in terms of temperature and time of exposure, whereas mechanical loading was described solely in terms of the distributed occlusal force. In addition, the influence of interfacial friction along the cavo-surface boundary was considered in terms of the coefficient of friction.

Based on results from the ANOVA, both occlusal and thermal loads had significant influence on the stress distribution within the restored molar. Thermal expansion of the amalgam resulting from elevated temperatures had significant effects on the normal stress which develops parallel to the pulpal floor (σ_{11})

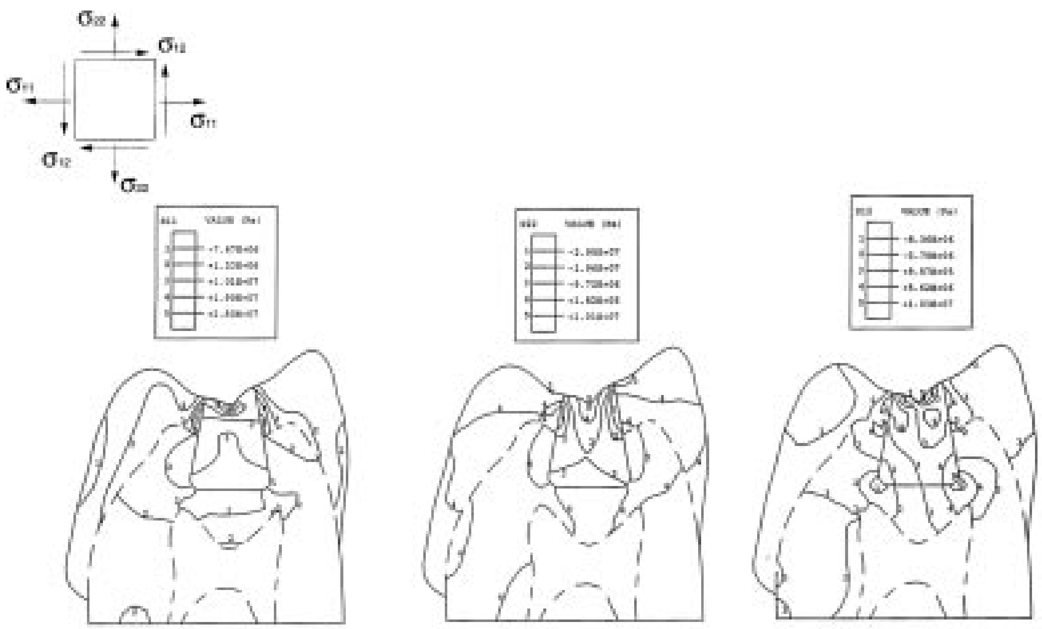

Figure 5 The influence of interfacial bonding on the stress distribution. ($T = 55\,^{\circ}\mathrm{C}, t = 5\,\mathrm{s}, P = 100\,\mathrm{N}, \mu = 0.5$) (a) σ_{11}, (b) σ_{22}, (c) σ_{12}. The dashed line is used to distinguish the boundary between the enamel, dentin and pulp.

as evident from Fig. 4a. However, thermal loading had far less influence on the remaining stress components as evident from Table IV. The distributed occlusal load was the primary variable affecting the in–plane stress components σ_{22} and σ_{12}, and also the out of plane stress σ_{33}. Over the range of temperatures and occlusal forces examined in this study, masticatory loading accounted for nearly 60% of the variation in maximum principal stress. Although the effects of temperature were secondary, thermal loading also resulted in significant changes in the maximum principal stress. Combined, these two oral factors comprised nearly 95% of the total change in maximum principal stress with parametric variation. It is important to note that the stress distribution in this study resulting from a superposition of mechanical and thermal loading is considerably higher than that reported in similar numerical investigations [5–7]. However, note that previous investigations examined the influence of mechanical loading on the stress distribution in molars with amalgam restorations, independent of thermal effects. Based on results from this numerical study, a superposition of mechanical and thermal loading is an important consideration in the evaluation of new cavity designs and restorative materials. Furthermore, effects from coefficient of thermal expansion mismatch between the restorative and biological materials on the stress distribution in restored teeth are significant.

In contrast to the effects from occlusal force and temperature, the time of thermal loading and cavo-surface boundary friction had far less influence on the stress distribution within either the tooth or restoration. The duration of thermal loading had the most influence on σ_{33} due to the plane strain boundary conditions and consequent suppression of free thermal expansion which occurs with prolonged conduction. Nevertheless, the duration of thermal loading had minimal influence on the maximum principal stress as evident from results of the ANOVA presented in Table IV. Similarly, cavo-surface margin friction had limited effects on the stress distribution which resulted within the restored molar. Variations in the friction coefficient may result from the use of specific methods of cavity preparation to promote marginal tabbing. However, efforts to increase interfacial friction and consequently promote interdigitation of amalgam has limited influence on the overall stress distribution of an imperfect joint. As the majority of amalgam restorations are not perfectly bonded, efforts to increase the degree of interdigitation along the cavo-surface boundary seem to provide little reward in reducing the magnitude of principal stress.

To further examine the influence of cavo-surface margin conditions, perfect bonding was introduced in the finite element model between the crown and amalgam. The influence of oral conditions described by the high level orthogonal design array listed in Table III were re-

T A B L E V The stress distribution within the restored molar for oral conditions of the high level orthogonal array with complete marginal bonding

Experiment	Temperature (°C)	Time (s)	Occlusal load (N)	Interface (μ)	σ_{11} (MPa)	σ_{22} (MPa)	σ_{33} (MPa)	σ_{12} (MPa)	σ_1 (MPa)
1	55	10	200	tied	3.77	− 1.14	− 8.51	16.42	17.92
2	55	1	0	tied	1.40	1.28	− 6.82	13.80	15.14
3	55	5	100	tied	2.73	0.31	− 7.63	15.90	17.47
4	5	5	200	tied	1.38	− 3.89	− 6.33	0.63	1.45
5	5	10	0	tied	− 0.70	− 1.01	− 4.74	− 0.49	− 0.34
6	5	1	100	tied	0.80	− 1.84	− 7.53	1.51	1.49
7	30	1	200	tied	2.70	− 2.31	− 7.31	9.20	9.73
8	30	5	0	tied	0.46	0.25	− 6.85	6.77	7.13
9	30	10	100	tied	1.54	− 1.07	− 6.63	7.96	8.30

evaluated assuming that the entire margin was perfectly bonded. Perfect bonding may be promoted with the use of an adhesive system. The resulting maximum stress within the restored molar is listed in Table V. In comparison with the maximum stress reported for the high level array in Table III, considerable differences are apparent between perfect and imperfect interfacial bonding. A reduction in crown temperature below ambient conditions ($T = 37\,^{\circ}\mathrm{C}$) resulted in a significant reduction of the maximum stress due to thermal contraction of the amalgam. However, the maximum principal stresses for the restoration with bonded margins in Table V resulting from elevated oral temperatures are very similar in magnitude to those resulting from unbonded margins listed in Table III. The distribution of σ_{11}, σ_{22}, and σ_{12} resulting from a 100 N occlusal load and crown temperature of 55 °C (Experiment 3 of the high level array in Table V) are shown in Fig. 5 (a–c), respectively. Note the increase in shear stress (σ_{12}) resulting from cavo-surface bonding in Fig. 5c in relation to the shear shress distribution resulting from no bonding previously shown in Fig. 4c. In addition, the reduction in normal stress (σ_{11} and σ_{22}) with cavo-surface bonding is also clearly apparent from a comparison of Figs 4 and 5. A number of investigators have distinguished the advantage of cavo-surface bonding in reducing the maximum stress in restored teeth that results during mastication [9, 31–32]. In fact, amalgam bonding has been proposed as a means of preventing cusp fracture through the reduction in maximum principal stress. However, results from the present study clearly show that marginal bonding of amalgam restorations may be detrimental when subjected to thermal loads. Adhesive bonding of the amalgam does not serve to reduce the maximum stress during mastication when subjected to elevated temperatures.

To further distinguish the influence of interfacial bonding on the influence of the remaining oral parameters, an ANOVA was conducted with the stress components in Table V. The normal stress components σ_{11}, σ_{22}, and σ_{33} were found to be nearly independent of the change in crown temperature. However, the shear stress was primarily influenced by thermal loading which accounted for over 90% of the observed variation. Consequently, based on the relationship between the shear and principal stress apparent in Equation 1, the maximum principal stress is also primarily a function of temperature. Thermal loading of the crown accounted for over 90% of the variation in σ_1 when cavo-surface bonding was present. High shear stresses along the amalgam/dentin and amalgam/enamel interfaces result from thermal expansion mismatch. According to results from the ANOVA, shear stresses resulting from thermal expansion mismatch are nearly independent of the time of thermal loading. Therefore, the interfacial shear stress resulting from thermal loading must contribute to adhesive failure in amalgam restorations. Although adhesive bonding can reduce stresses induced by occlusal forces, cavo-surface bonding of amalgam restorations does not reduce the maximum principal stress which results from thermal loading.

Results obtained from the finite element analysis have conveyed the significance of thermal loading to the stress distribution which develops within restored molars. The influence of cavo-surface bonding on the stress distribution and detrimental effects of marginal bonding to the stress that results from thermal loading of molars with amalgam restorations were also distinguished. Simultaneous mechanical and thermal loading is a clinically relevant oral condition which promotes stresses which are significantly different from that resulting solely from occlusal loading. However, the magnitude of maximum tensile stress resulting from simultaneous mechanical and thermal loading did not significantly exceed that which has been reported in related studies restricted to mechanical loading. Therefore, it appears from the numerical results that tooth fracture occurs as a result of damage accumulation. Indeed, Bell *et al.* [32] also suggested that cusp fracture was the result of progressive crack propagation in regions of high tensile stress. Based on his numerical assessment of the stress distribution which results from occlusal loading, it was suggested that marginal bonding could be used to suppress crack propagation through a reduction in stress. However, results from the present study clearly indicate that marginal bonding promotes the development of tensile stress within teeth with amalgam restorations and would not serve to suppress crack growth. Therefore, the mechanisms of cyclic crack propagation in restored molars and effects of the restorative material on the rate of crack growth will be the topic of future investigations.

5. Conclusions

A finite element analysis of a restored mandibular molar with standard Class II amalgam preparation was conducted. In particular, the stress distribution resulting from a superposition of simultaneous mechanical and thermal loading was determined. The influence of crown temperature, duration of thermal loading, occlusal force, and cavo-surface margin conditions were identified through an experimental design and analysis of variance. Based on the results from this numerical study, the following conclusions were drawn;

1. Over the range in oral conditions considered in this study, the maximum principal stress occurred in the dentin at the junction of the pulpal floor and lingual surface margin. The maximum principal stress resulting from all conditions considered was found to be 20 MPa.
2. Although the effects of temperature on the maximum principal stress were secondary to those of occlusal force, thermal loading resulted in significant changes in the stress distribution. Thermal loads were found to be most influential on the normal stress which develops parallel to the pulpal floor and consequently accounted for over 35% of the variation in the maximum principal stress. The maximum principal stress occurred at the junction of the pulpal floor and cavo-surface margin, regardless of the oral conditions.
3. The duration of thermal loading and the coefficient of friction (μ) along the cavo-surface margin had minimal influence on the magnitude of maximum principal stress resulting from either mechanical or thermal loading.

4. An examination of the stress distribution that results from perfect bonding between the crown and amalgam indicated that thermal loading promotes the development of significant shear stress across the lingual and buccal margins. Consequently, the maximum principal stress resulting from thermal loading was found to be nearly equivalent to that which occurs with imperfect bonding. Perfect bonding along the cavo-surface margin does not provide a reduction of principal stress under conditions of thermal loading. In fact, thermal loading undoubtedly contributes to the degradation of adhesive bonds introduced along the cavo-surface margin.

5. Due to the clinical relevance, a superposition of mechanical and thermal loading should be considered in the evaluation of new cavity designs and/or restorative materials.

Acknowledgments

The authors would like to acknowledge partial support from the University of Maryland Baltimore County through a Designated Research Initiation Fund. Many thanks are also extended to Rick Mori and Derek Brown from the University of Maryland School of Dentistry for their support and encouragement.

References

1. H. LETZEL, M. A. VAN'T HOF, M. M. A. VRIJHOEF, G. W. MARSHALL and S. J. MARSHALL, *Dent. Mater.* **5** (1989) 115.
2. B. V. BRALY and E. H. MAXWELL, *J. Prosthet. Dent.* **45** (1981) 411.
3. D. B. MAHLER, *J. Dent. Res* **37** (1958) 516.
4. E. W. JOHNSON, C. R. CASTALDI, D. J. GAU and G. P. WYSOCKI, *ibid.* **47** (1968) 548.
5. C. RUBIN, N. KRISHNAMURTHY, E. CAPILOUTO and H. YI, *ibid.* **62** (1983) 82.
6. J. H. P. DE VREE, M. C. R. B. PETERS and A. J. M. PLASSCHAERT, *ibid.* **63** (1984) 1217.
7. I. R. SPEARS, R. VAN NOORT, R. H. CROMPTON, G. E. CARDEW and I. C. HOWARD, *ibid.* **72** (1993) 1526.
8. D. L. MORIN, W. H. DOUGLAS, M. CROSS and R. DELONG, *Dent. Mater.* **4** (1988) 41.
9. M. C. R. B. PETERS and H. W. POORT, *J. Dent. Res.* **62** (1983) 358.
10. E. K. HANSEN, *Dent. Mater.* **4** (1988) 170.
11. R. B. JOYNT, G. WEICZCOWSKI, R. KLOCKOWSKI and E. L. DAVIS, *J. Prosthet. Dent.* **57** (1987) 431.
12. L. L. STAMPALIA, J. I. NICHOLS, J. S. BRUDVIK and D. W. JONES, *ibid.* **55** (1986) 694.
13. J. H. PURK, J. D. EICK, E. J. DESCHEPPER, R. P. CHAPPELL and D. E. TIRA, *Quint. Int.* **21** (1990) 545.
14. W. S. BROWN, W. A. DEWEY and H. R. JACOBS, *J. Dent. Res.* **49** (1970) 752.
15. TH. A. M. SPIERINGS, J. H. P. DE VREE, M. C. R. B. PETERS and A. J. M. PLASSCHAERT, *ibid.* **63** (1984) 1096.
16. J. H. P. DE VREE, TH. A. M. SPIERINGS and A. J. M. PLASSCHAERT, *ibid.* **62** (1978) 756.
17. H. R. JACOBS, R. E. THOMPSON and W. S. BROWN, *ibid.* **52** (1973) 248.
18. B. A. LLOYD, M. B. MCGINLEY and W. S. BROWN, *ibid.* **57** (1978) 571.
19. I-DEAS, Masters Series 2.0, (Structural Dynamics Research Corporation, Ohio, 1990).
20. B. S. KRAUS, R. E. JORDAN and L. ABRAMS, in ''A study of the masticatory system: Dental anatomy and occlusion'' (Williams and Wilkins Company, Baltimore, 1969).
21. R. S. SCHWARTZ, J. B. SUMMIT and J. W. ROBBINS, in ''Fundamentals of operative dentistry'' (Quintessence Publishing, Chicago, 1996).
22. B. VAN MEERBEEK, G. WILLEMS, J. P. CELIS, J. R. ROOS, M. BRAEM, P. LAMBRECHTS and G. VANHERLE, *J. Dent. Res.* **72** (1993) 1434.
23. R. W. THRESHER and G. E. SAITO, *J. Biomech.* **6** (1973) 443.
24. W. J. O'BRIEN, in ''Dental materials and their selection'', 2nd Edn (Quintessence Publishing, Chicago, 1997).
25. L. G. WATANABE, G. W. MARSHALL and S. J. MARSHALL, *Dent. Mater.* **12** (1996) 109.
26. Abaqus, Version 5.7 (K. A. S. Hibbit Inc., Rhode Island, 1998).
27. J. F. BATES, G. D. STAFFORD and A. HARRISON, *J. Oral Rehabil.* **2** (1975) 349.
28. W. S. BROWN, R. E. THOMPSON and H. R. JACOBS, *J. Dent. Res.* **51** (1972) 461.
29. E. P. POPOV, in ''Mechanics of materials'', 2nd Edn (Prentice Hall Publ., New Jersey, 1978) p. 240.
30. C. R. HICKS, in ''Fundamental concepts in the design of experiments,'' 4th Edn (Oxford University Press, Oxford, 1993) p. 217.
31. D. L. MORIN, M. CROSS, V. R. VOLLER, W. H. DOUGLAS and R. DELONG, *Dent. Mater.* **4** (1988) 77.
32. J. G. BELL, M. C. SMITH and J. J. DE PONT, *Aust. Dent. J.* **27** (1982) 283.

Received 6 November 1998
and accepted 7 December 1998